

Raman spectroscopy of complex defined media: Biopharmaceutical applications

F.R. Hajiyeva^{1*}, N.A. Abdullayev²

¹ *Research Institute of Obstetrics and Gynecology, 118 Kazim Kazimzadə Str., Baku AZ1065, Azerbaijan*

² *Institute of Physics, Azerbaijan National Academy of Sciences, 131 H.Javid Ave., Baku AZ1143, Azerbaijan*

**For correspondence: dr.fatima79@mail.ru*

Received: May 14, 2021; Received in revised form: June 12, 2021; Accepted: June 19, 2021

Hamster ovary cells were grown in a batch culture flask for 10 days in an incubator maintained with 5% CO₂ and 37 °C temperature. The 2 ml supernatant was collected each day, in duplicate, and was stored in a freezer at -20 °C. Concentrations of glucose and lactate were estimated, in the supernatant, on an HPLC machine, and the same sample was used to immediately obtain the results of Raman measurements. We demonstrate the detection of glucose and lactate concentrations with high accuracy in the supernatants of hamster ovary (HO) cell culture, grown in shake flasks in batch fermentation mode, using Raman spectroscopy and explicit model-based classical least squares (CLS) algorithm. A deterministic Raman spectral library of pure components was created by acquiring Raman spectra from credible nutrient media constituents and HO cell culture metabolites. Only analyzers present with concentrations above the instrument's detection limit were included in this library. Residuals obtained after CLS analyses were used to identify missing components and to generate a revised library. An algorithmic sieve was thus, construed to obtain an appropriate Raman spectral library from a complex chemical mixture that is well-defined but an industrial secret. High performance liquid chromatography (HPLC) was used to provide reference glucose and lactate concentrations. We demonstrate the detection of glucose and lactate concentrations in the supernatants of HO cell culture using Raman spectroscopy and explicit model-based CLS analysis.

***Keywords:** Raman spectroscopy, bioreactors, classical least squares, glucose detection, lactate detection*

INTRODUCTION

Real time monitoring and control of bioprocesses are essential in improving their efficiency and reducing the cost of the final product. With the advancement of biotechnology, bypasses are no longer restricted to the production of alcohols, organic and amino acids, and small biomolecules such as insulin, enzymes, and some antibiotics. Now, they are also a method of choice for using modified cell culture expression systems and the production of large biomolecules such as monoclonal antibodies that include some vaccines for human use (Zhu, 2012).

Among the mammalian cell culture expression systems, the relatively high robustness of hamster ovary (HO) cells in different bioreactor systems is well established. Furthermore, HO cells

are very efficient in posttranslational glycosylation of proteins, making them closely resemble human glycosylation patterns in order to avoid or to reduce the immune responses after drug administration. Some examples of such proteins are follicle stimulating (Yamamoto et al., 2011; Whelan et al., 2012).

To enhance the technologies available for monitoring and control of environmental parameters in bioreactors, several optical and spectroscopic modalities have been investigated as they are non-invasive and provide information in real time. Raman spectroscopy is one of the most promising techniques in this regard. It is based on the inelastic scattering of light and provides a biochemical fingerprint for the sample under investigation.

High chemical specificity of Raman spectroscopy is the result of its measurement of vibrational energies in chemical bonds. Near infrared (NIR) laser excitation helps to minimize luminescence background generated either from the substrate or from the biological sample being probed. It also has a higher penetration depth of biological materials and less tissue damage at a higher excitation power compared with visible excitation. Miniaturization and integration of Raman technology are highly desirable, and in recent years, there has been an increase in efforts in this direction (Abu-Absi et al., 2011; Li et al. 2010).

Raman spectroscopy coupled with Chemometrics has recently been used for real time monitoring and simultaneous prediction of multiple culture parameters including glutamine, glutamate, glucose, lactate, ammonium, viable cell density, and total cell density in HO cell culture bioreactors. It has also been used for the rapid identification, characterization, and quality assessment of complex cell culture media components used for industrial mammalian cell culture. But, all of the studies have used implicit models, where reference measurements on a training sample set are performed to acquire information about the system to be investigated. A model is thus constructed, based on the training set, which implicitly accounts for any physical effects that influence the measured Raman spectra, allowing concentration estimation of unprocessed samples. However, the training samples are system specific and only model the particular system under investigation.

They are not generally applicable to other systems. Implicit models do have utility and validity in bioprocess supervision applications, where the same bioreaction is to be repeatedly monitored for production purposes, but they have limited utility in bioprocess development applications where variations in operating conditions, growth rates, and medium composition are a necessary requirement.

Explicit methods, based on physical modeling the system to be analyzed, are preferred for bioprocess development applications. 161 Explicit models have previously been used to estimate the ethanol concentration in Baker's yeast fermentation and classical least-squares (CLS) fitting was used to estimate glucose and spiked quantities of glutamine, lactate, and ammonia, in filtered samples of a bioreactor (Lee et al., 2004; Shope et al., 1987).

The industrial mammalian cell culture requires complex nutrient media components. Chemically defined media components are preferred to avoid unknown parameters and subsequently facilitate the regulatory approval of the product. The exact composition of the nutrient media in most cases is kept an industrial secret. Hence, it is not straightforward to use explicit methods such as CLS analysis for the prediction of metabolite concentrations.

In this article, we have shown that explicit model-based CLS algorithm can be used to detect mammalian (HO) cell culture metabolites (glucose and lactate) with high accuracy using NIR Raman spectroscopy. An algorithmic sieve was construed and an appropriate Raman spectral library obtained from a complex chemical mixture that is well-defined but kept confidential by respective pharmaceutical industries. High performance liquid chromatography (HPLC) was used to obtain reference concentrations of glucose and lactate.

MATERIALS AND METHODS

Mammalian cells. Hamster ovary cells were grown in a batch culture flask for 10 days in an incubator maintained with 5% CO₂ and 37 °C temperature. Similarly, HO cells were batch cultured for 13 days. The 2 ml supernatant was collected each day, in duplicate, and was stored in a freezer at -20°C. Concentrations of glucose and lactate were estimated, in the supernatant, on an HPLC machine, and the same sample was used to obtain Raman measurements immediately.

Confocal near infrared Raman spectroscopy system. Short description of spectroscopy: Raman scattering studies were carried out on a three-dimensional confocal Raman microspectrometer Nanofinder 30 (Tokyo Instr.), Excitation wavelength $\lambda=532$ nm. The radius of the cross section of the incident laser beam was approximately 4 μ m. The investigations were carried out in the geometry of backscattering. The radiation receiver was a cooled CCD camera (-70°C) operating in the photon counting mode. All measurements are taken at an exposure time of 1 second and an excitation

Table 1. Comparison of explicit and implicit calibration models

Whelan et al. Partial least (implicit)	This work Partial least squares (PLS) [leave-one-out cross validation (LOOCV)]					
	R ²	Standard error	R ²	Standard error	R ²	Standard error
Glucose	0.91	2.09	0.99	2.4	0.98	3.5
Lactate	0.99	11.49	0.99	3.1	0.99	5.2

Table 2. List of constituents present in hamster ovary cell culture nutrient media (adapted from Schröder et al. (2004))

Inorganic salts	Molar concentration (mM)	Carbohydrates	Molar concentration (mM)
CaCl ₂	1.9	d-Glucose	34
CuSO ₄ ·5H ₂ O	4.81x10 ⁻⁶	I-Amino acids	0.377
FeSO ₄ ·7H ₂ O	1.20x10 ⁻³	I-Alanine	0.879
KNO ₃	9.02x10 ⁻⁴	I-Arginine·HCl	0.267
KCl	6.51	I-Asparagine·H ₂ O	0.31
MgSO ₄	0.576	I-Cysteine-HCl·H ₂ O	0.349
NaCl	52	I-Cysteine·2HCl	0.652
NaHCO ₃	48.8	I-Glutamic acid	7.2
Na ₂ HPO ₄	0.4	I-Glutamine	0.52
NaH ₂ PO ₄ ·H ₂ O	1.25	Glycine	0.28
Na ₂ SeO ₃ ·5H ₂ O	9.98x10 ⁻⁵	I-Histidine·HCl·H ₂ O	0.973
ZnSO ₄ ·7H ₂ O	1.20x10 ⁻³	I-Isoleucine	1
		I-Leucine; I-Lysine·HCl	1.04
Vitamins and miscellaneous compounds			
dl-Pantothenic acid, calcium salt	1.09x10 ⁻²	I-Methionine	
Choline chloride	7.44x10 ⁻²	I-Phenylalanine	
Ethanolamine	0.02	I-Proline	
Folic acid	1.21x10 ⁻²	I-Serine	
Hypoxanthine	0.1	I-Threonine	
l-Inositol	8.79x10 ⁻²	I-Tryptophan	
Linoleic acid	1.20x10 ⁻⁴	I-Tyrosine comma>disc	
Lipoic acid	4.07x10 ⁻⁴	I-Valine	
Methotrexate (MTX) ^b			
Nicotinamide	1x10 ⁻⁴ to 0.1		
Phenol red	3.94x10 ⁻²		
Pluronic F-68c	5.21x10 ⁻²		
Pyridoxal·HCl	2.36x10 ⁻²	Peptones and proteins	
Pyridoxine·HCl	1.21x10 ⁻⁴	Fetuid	
Riboflavin	1.32x10 ⁻³	Insulin	
Sodium pyruvate	2.51	Holo-Transferrin	
Thiamine·HCl	1.46x10 ⁻²	Casein peptone	
Thymidine	0.016	Soybean flour peptone	
Vitamin B12	4.13x10 ⁻⁴	Soybean flour brothe	

CLS analysis. Because the exact composition of HO cell culture nutrient medium is kept confidential by respective pharmaceutical industries, we decided to select nutrient media constituents and HO cell culture metabolites from a reliable literature. For example, Table 1 by Schröder et al., provides information in this regard and is used to develop the Raman spectral library (Schröder et al.,

2004). This table is shown in Fig. 1. We initially selected only those constituents from Fig. 1, which were known to generate Raman spectra (for example, the inorganic salts do not show Raman spectra as they dissociate into ions in an aqueous solution) and were present in concentration above the Raman instrument detection limit of ~1 mM. Because several of the amino acids mentioned in Table 1

have concentration reaching 1 mM, we selected the ones with high Raman cross section. Zhu et al. provide in detail the Raman spectra of amino acids in solution (Zhu et al., 2011).

A deterministic Raman spectral library of pure components was thus obtained from credible nutrient media constituents and HO cell culture metabolites and was used as a calibration routine for the CLS analysis. Phosphate buffered saline (PBS) was used to prepare all pure component solutions. Raman spectra were acquired from each day's supernatant. Polynomial fitting was not used to estimate and remove fluorescence background from Raman spectra before using the CLS analysis and performing concentration prediction for glucose and lactate. Cosmic rays were removed from the Raman spectra, and fifth order smoothing using Savitzky-Golay algorithm was performed using MATLAB to suppress noise. The Raman spectra were normalized with respect to the CLS coefficient of water. It was also taken care that the concentration prediction of all basis spectra constituents generates non-negative numbers. A final Raman spectral library was thus conceived. Using CLS calibration routine developed with this Raman spectral library, concentrations of glucose and lactate were predicted. HPLC was used to obtain reference concentrations of glucose and lactate.

Underlined constituents were part of the Raman spectral library used for classical least squares (CLS) calibration routine development (Schroder et al., 2004).

Calculated as the root mean-squared error of predication, using Raman-predicted concentration values and HPLC-generated reference concentration values.

RESULTS AND DISCUSSION

The Raman spectral library, which was obtained after implementing the algorithmic sieve, is shown in Fig. 2. In the process of obtaining this library, some constituents that were mentioned as ~1 mM concentration in Fig. 1 such as L-leucine and L-valine were removed. Their presence made the concentration predictions worse and also the CLS fit to the supernatant Raman spectrum- produced residuals with structure. Removing any of the Raman spectra present in spectral library of Fig. 2 made the concentration predictions worse as did

the addition of spectra from additional constituents. Thus, a final Raman spectral library for CLS analysis was conceived.

Raman spectra of L-arginine HCl, glucose, L-threonine, L-valine, sodium pyruvate, sodium bicarbonate, glycine, and sodium lactate were acquired at 20 mM concentration each in PBS. Raman spectra of PBS and water were also acquired and included in the Raman spectral library.

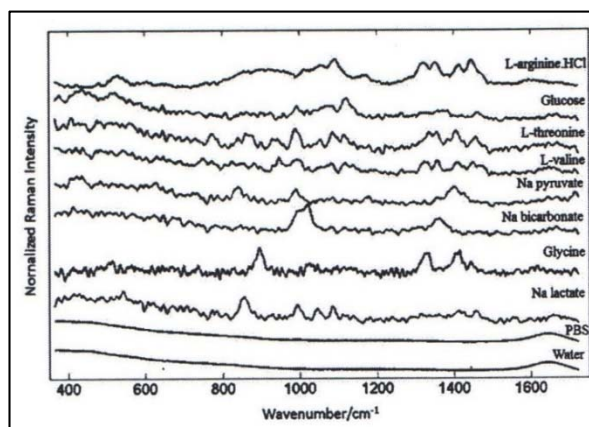


Fig. 1. Raman spectral library consisting of pure components; some selected from hamster ovary cell culture constituents mentioned in Fig. 1. PBS, phosphate buffered saline.

In Fig. 1, the Raman spectrum of water has been subtracted from each of the solute Raman spectrum for better visualization. The main Raman peaks and bands observed in the spectra of pure components mentioned in Fig. 2 are listed in Table 2. A broad Raman peak at 1641 cm^{-1} was observed in the Raman spectrum of water, and a weak Raman peak at 992 cm^{-1} was observed in the Raman spectrum of PBS.

The detection limit of sodium lactate and D-glucose aqueous solutions is shown in Fig. 3, using the NIR Raman spectroscopy system. Here, we define the detection limit as noise equivalent concentration, i.e. the concentration at which $SNR = 1$. It was found that the detection limit of sodium lactate is better than 3 mM (obtained after extrapolation of curve), while that of D-glucose is better than 2 mM. The data in this figure were an average of three measurements, and the error bars were smaller than the shown size of data points.

Table 3. Main Raman peaks (Raman shift cm^{-1}) observed in the Raman spectra of pure components mentioned in Fig.1. Water exhibited a broad Raman peak at 1641 cm^{-1} white phosphate buffered saline (PBS) at 992 cm^{-1}

L-arginine HCl	Glucose	L-threonine	L-valine	Na pyruvate	Na bicarbonate	Clycine	Na lactate
-	435	-	-	-	-	-	-
-	516	-	-	-	-	-	-
530	-	-	-	-	-	-	-
-	-	-	750	-	-	-	-
-	-	771	-	-	-	-	-
-	-	-	-	840	-	-	-
-	-	-	-	-	-	-	855
-	-	861	-	-	-	-	-
-	-	-	-	-	-	897	-
919 (broad)	-	-	-	-	-	-	-
-	-	-	946	-	-	-	-
-	990	990	991	991	-	-	992
-	-	-	-	-	1027	-	-
-	-	-	-	-	-	-	1045
-	-	1055	-	-	-	-	-
-	1076	-	-	-	-	-	-
-	-	1085	1084	-	-	-	1085
1091	-	-	-	-	-	-	-
-	-	1112	-	-	-	-	-
-	1121	-	-	-	-	-	-
1172	-	-	-	-	-	-	-
1324	-	-	1324	-	-	-	-
-	-	1335	-	-	-	1333	-
1356	-	-	1358	-	1361	-	-
-	1374	-	-	-	-	-	-
-	-	-	-	1401	-	-	-
1415	-	1409	1412	-	-	1413	-
1453	1460	1456	1455	-	-	-	1456

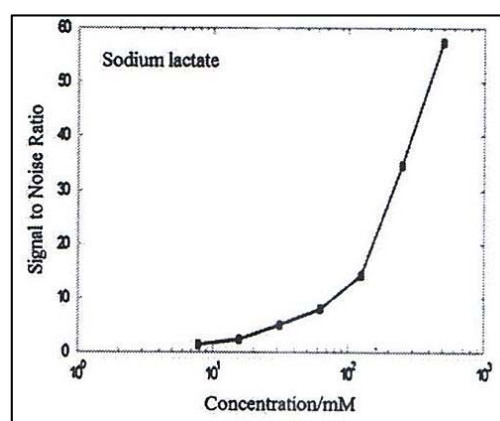
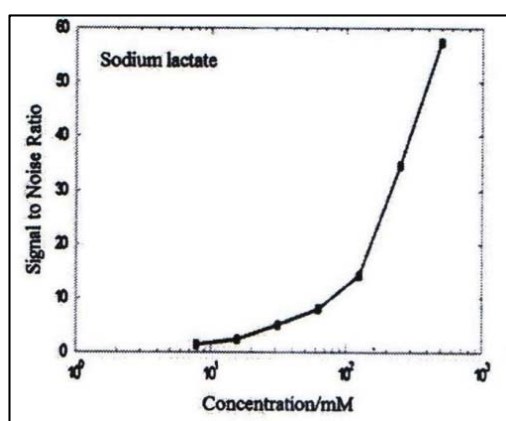


Fig. 2. Detection limit of sodium lactate and D-glucose solutions measured using near infrared (NIR) Raman spectroscopy system. Error bars were smaller than the shown size of data points. For D-glucose, the mean of area under Raman peak at 1121 cm^{-1} was used for signal calculation, while for sodium lactate, the mean of area under Raman peak at 855 cm^{-1} was used.

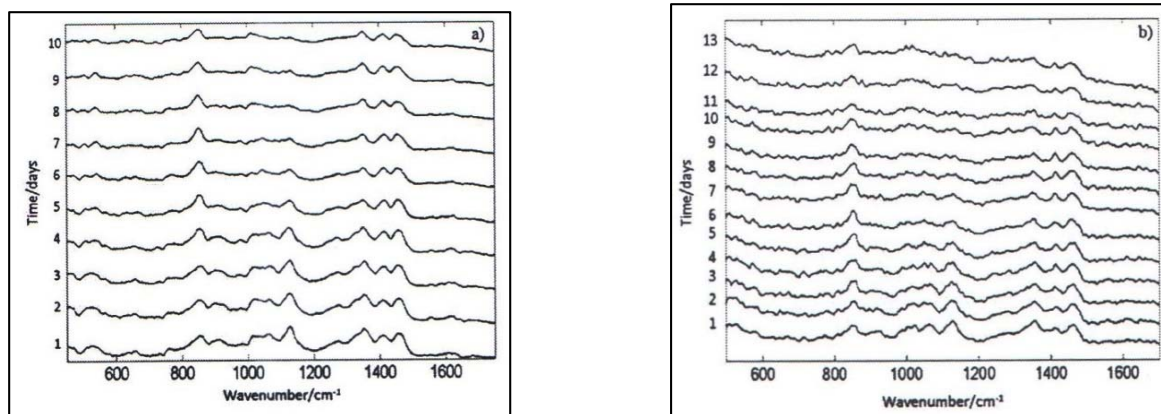


Fig. 3. Raman spectra obtained from hamster ovary cell culture supernatants using (a) Invitrogen cell line and (b) Sanofi cell line during 10 and 13 days of shake flask culture, respectively, in batch mode.

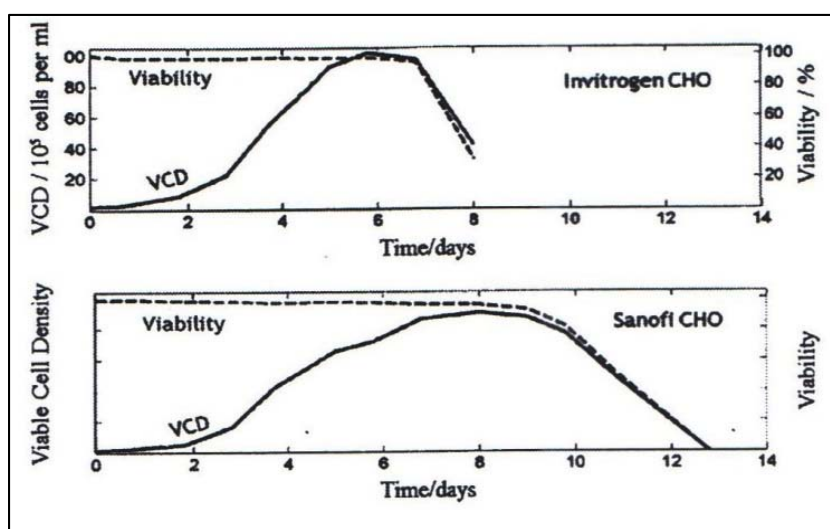


Fig. 4. Growth curves for Invitrogen and Sanofi hamster ovary cell cultures. Sanofi cell line is optimized for antibody production and hence has a longer stationary phase. VCD, viable cell density.

Each measurement consisted of ten spectral acquisitions. For D-glucose, the mean of area under Raman peak at 1121 cm^{-1} was used for signal calculation, while for sodium lactate, the mean of area under Raman peak at 855 cm^{-1} was used. Median standard deviation across the whole Raman spectrum of ten Raman spectra was used for noise estimation.

Figure 4(a) shows the Raman spectra obtained from Invitrogen HO cell culture supernatants on each of the 10 days, while Fig. 4(b) shows the same for Sanofi HO cell culture supernatants for 13 days.

PBS Raman spectrum has been subtracted from each day's supernatant Raman spectrum for better visualization. The difference in Raman spectra on each day can clearly be observed. Main Raman peaks at 853 cm^{-1} , 900 cm^{-1} (broad), 1021 cm^{-1} , 1064 cm^{-1} , 1128 cm^{-1} , 1276 cm^{-1} , 1352 cm^{-1} , 1412 cm^{-1} , and 1458 cm^{-1} were observed.

The growth curves for Invitrogen and Sanofi HO cell cultures respectively are shown in Fig. 5. The Sanofi HO cell culture has a longer stationary phase because it has been optimized for antibody production.

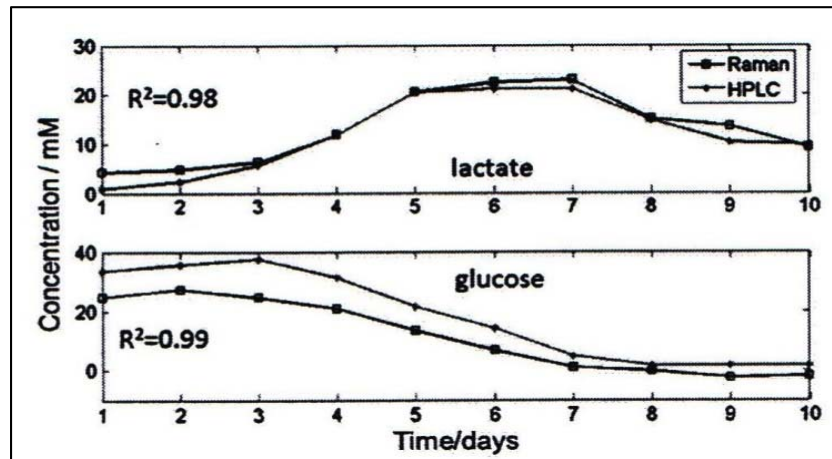


Fig. 5. Prediction of glucose and lactate concentrations in invitrogen hamster ovary cell culture supernatants using Raman spectroscopy and explicit model-based classical least squares (CLS) analysis. The error bars were equivalent to 2 mM concentration for Raman measurements and 0.5 mM concentration for high performance liquid chromatography (HPLC) measurements (Abu-Absi et al., 2011).

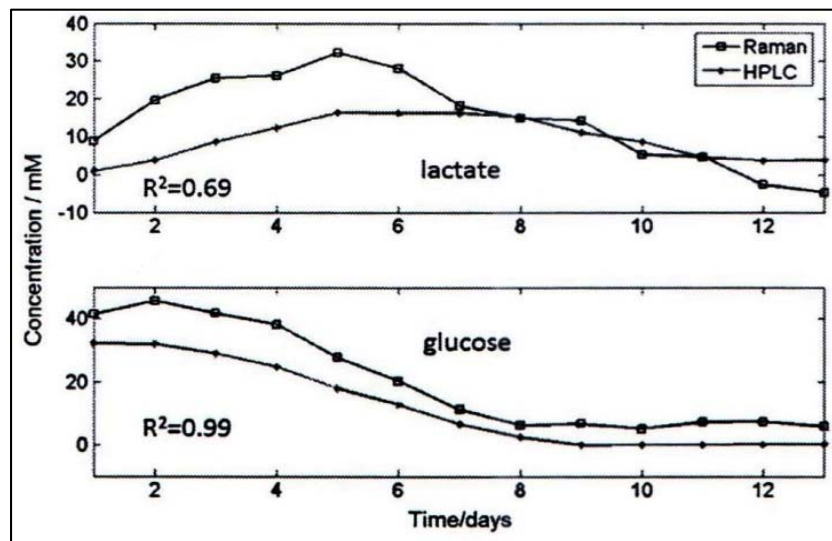


Fig. 6. Prediction of glucose and lactate concentrations in Sanofi hamster ovary cell culture supernatants using Raman spectroscopy and explicit model-based classical least squares (CLS) analysis. HPLC, high performance liquid chromatography (Abu-Absi et al., 2011).

Figure 6 shows the glucose and lactate concentration prediction in Invitrogen HO cell culture supernatants using Raman spectroscopy and explicit model-based CLS algorithm. Comparison with reference concentration values obtained using HPLC is also shown. The experiment was per-

formed three times, and average values of measurement are plotted. The error bars were equivalent to 2 mM concentration for Raman measurements and 0.5 mM concentration for HPLC measurements. The time required for glucose and lactate concentration measurements using HPLC was about 45 min per sample, after the HPLC was calibrated

with the correct measurement column. Calibration of HPLC with a new column required almost 2h. Because the same column could not be used for glucose/lactate and amino acids, for example, HPLC was found to be labor intensive. On the other hand, time required for Raman measurements was about 8 min per sample after the charged coupled device camera of NIR Raman system had been cooled to -90 °C. Cooling of the camera required about an hour. But once ready, the Raman system could be used to predict concentrations of multiple analytes from a single spectral measurement.

We also used an implicit calibration model and performed partial least squares (PLS) analysis using the Invitrogen HO cell culture supernatant Raman spectra from 10 days and the reference concentrations provided by HPLC. The results of leave-one-out cross validation are shown in Table 1. In comparison with Whelan et al. it is observed that the correlation in glucose and lactate concentration predictions obtained using implicit calibration model is comparable, but the standard error for lactate concentration prediction is significantly less in our case. The correlation in concentration prediction using CLS is also comparable with slightly higher standard errors of prediction compared with PLS.

In Fig. 4, we show the glucose and lactate concentration prediction in Sanofi HO cell culture supernatants using Raman spectroscopy and explicit model-based CLS algorithm. Comparison with reference concentration values obtained using HPLC is also shown. The slightly different prediction results for lactate in Figs 5 and 6 are because of the fact that we had used the same smoothing and basis spectra-based CLS model for both Invitrogen and Sanofi cell lines. These cell lines have different metabolism, as shown in Fig. 5, and the CLS algorithm can be sensitive to high frequency system noise or experimental noise because of the pseudo-inversion of the measurement matrix. One way to improve this in the future would be to introduce techniques such as regularization.

CONCLUSIONS

We have shown for the first time that the detection of glucose and lactate concentrations with high accuracy is possible in HO cell culture supernatants using Raman spectroscopy and explicit

model-based CLS algorithm. This corresponds to the data obtained by Yamamoto Y.S. et al. (Yamamoto Y.S. et al. (2011)). When exact composition of the nutrient media is unknown, a deterministic Raman spectral library of pure components can be created by acquiring Raman spectra from credible nutrient media constituents and HO cell culture metabolites. Residuals obtained after CLS analyses can be used to identify missing components or those present in excess. An algorithmic sieve thus generated provides a revised Raman spectral library that can be used for metabolite concentration predictions (Goh, 2013; Vogel, 2002). Other HO cell culture metabolites can also be monitored after improving the detection limit of the system, and it will require the use of respective HPLC columns to provide reference data values. Once validated, Raman spectroscopy-based concentration measurements require about an order of magnitude less time comparatively are not labor intensive and have the advantage of ease of automation (Lee et al., 2004). Singh et al. also describe this circumstance in their works (Schroder et al., 2004). We believe that our algorithm and approach can be used for rise of quality analytical technology. It also assists in the development of processes and promotes their intensification.

REFERENCES

- Abu-Absi N.R., Kenty B.M., Cuellar M.E. et al.** (2011) Real time monitoring of multiple parameters in mammalian cell culture bioreactors using an in-line Raman spectroscopy probe. *Biotechnol. Bioeng.*, **108(5)**: 1215. doi: 10.1002/bit.23023.
- Goh S.** (2013) Micro-bioreactor design for Chinese Hamster ovary cells. *PhD thesis*, Massachusetts Institute of Technology, Cambridge, MA, USA, p. 195-203.
- Lee H.L., Boccazzi P., Gorretb N. et al.** (2004) *In situ* bioprocess monitoring of Escherichia coli bioreactions using Raman spectroscopy. *Vib. Spectrosc.*, **35**: 131.
- Li B., Ryan P.W., Ray B.H. et al.** (2010) Final submitted version, not proof corrected. 1. Rapid characterization and quality control of complex cell culture media solutions using Raman spectroscopy and chemometrics. *Biotechnol. Bioeng.*,

- 107(2):** 290. doi: 10.1002/bit.22813.
- Schroder M., Matischak K., Friedl P.** (2004) Serum- and protein-free media formulations for the Chinese hamster ovary cell line DUKXB11. *J. Biotechnol.* **107(2):** 279. doi: 10.1002/bit.22813
- Shope T.B., Vickers T.J., Mann C.K.** (1987) The direct analysis of fermentation products by Raman spectroscopy. *Appl. Spectrosc.*, **47:** 908.
- Singh G.P., Goh S., Canzonier M. et al.** (2015) Raman spectroscopy of complex defined media: biopharmaceutical applications. *J. Raman Spectrosc.*, **40(6):** 545-550.
- Vogel C.R.** (2002) Computational methods for inverse problems (Frontiers in Applied Mathematics). *Soc for Industrial & Applied Math, Philadelphia, USA*, 183p.
- Whelan J., Craven S., Glennon B.** (2012) In situ Raman spectroscopy for simultaneous monitoring of multiple process parameters in mammalian cell culture bioreactors. *Biotechnol. Progr.* **28:** 1355. doi.org/10.1002/btpr.1590
- Yamamoto Y.S., Shinzawa H., Matsuura Y. et al.** (2011) Noninvasive subsurface analysis using multiple miniaturized Raman probes. Part I: Basic study of thin-layered transparent models of biomedical tissues. *Appl. Spectrosc.*, **65(8):** 844. doi: 10.1366/11-06245.
- Zhu G., Zhu X., Fan Q., Wan X.** (2011) Separation and screening of compounds of biological origin using molecularly imprinted polymers *Spectrochim. Acta A.*, **78:** 1187 doi: 10.1016/j.jchromb.2004.02.012.
- Zhu J.** (2012) Mammalian cell protein expression for biopharmaceutical production. *Biotechnol. Adv.*, **30(5):** 1158. doi: 10.1016/j.biotechadv.2011.08.022.

Mürəkkəb mühitlər üçün Raman spektroqrafiyası: biofarmakoloji tətbiq

F.R. Hacıyeva¹, N.A. Abdullayev²

¹ *Elmi-Tədqiqat Mamalıq və Ginkeologiya İnstitutu, Bakı, Azərbaycan*

² *AMEA-nın Fizika İnstitutu, Bakı, Azərbaycan*

Tədqiqat daxilində dağsiçanın yumurtalıq hüceyrələri kolbada yetişdirilərək 10 gün ərzində inkubatorada 5%-li CO₂ məhlulunda yetişdirilmişdir. Toplanmış 2ml supernatant 20°C dondurucu kamerada saxlanmışdır. Supernatantda qlükoza və laktatın konsentrasiyası yüksək effektivlikli maye xromatoqrafiyada təyin edilmişdir, eyni nümunə mühitin parçalanmanın kombinasiyasının ölçülməsi üçün də istifadə edilmişdir. Biz raman spektroqrafiyasından və klassik ən kiçik kvadrat modelindən istifadə etməklə dövrü fermentasiya rejimində kolbada yetişdirilən qlükoza və laktatın konsentrasiyasını təyin etdik. Dağsiçanın yumurtalıqlarının hüceyrələri kultur metabolitləri və qidalı mühitin təmiz komponentlərinin kombinasiyalı dağılma spektrlərinin əldə edilməsilə təmiz komponentlərinin kombinasiyalı dağılma spektrlərinin bazası yaradılmışdır. Bu bazaya yalnız cihazın təyin etdiyi həddən yuxarı olan analizatorlar daxil edilmişdir. Klassik ən kiçik kvadrat təhlilindən sonra alınan qalıqlar çatışmayan komponentlərin aşkar edilməsi və bazanın düzəldilməsi üçün istifadə edilmişdir. Belə ki, mürəkkəb kimyəvi qarışıqlardan kombinasiyalı dağılmanın spektral bazasının alınması üçün alqoritm yaradılmışdır. Etalon qlükoza və laktat konsentrasiyalarının alınması üçün yüksək effektivlikli maye xromatoqrafiyadan istifadə edilmişdir. Biz raman spektroqrafiyasının köməkliliylə dağsiçanın yumurtalıq hüceyrəsinin kulturlarının supernatantlarında qlükoza və laktatı təyin etdik.

Açar sözlər: Raman spektroskopiyası, bioreaktorlar, ən kiçik kvadratlar klassik metodu, qlükozanın aşkarlanması, laktatın aşkarlanması

**Рамановская спектроскопия для сложных сред: биофармацевтическое применение
Ф.Р. Гаджиева¹, Н.А. Абдуллаев²**

¹ *НИИ акушерства и гинекологии, Баку, Азербайджан*

² *Институт физики НАН Азербайджана, Баку, Азербайджан*

Клетки яичников хомяка в течение 10 дней выращивали в колбе, помещенной в инкубатор, где культивирование осуществлялось при 5%-ом CO₂ и температуре 37°C. Собранные 2 мл супернатанта хранились в морозильной камере при температуре 20°C. Концентрации глюкозы и лактата в супернатанте оценивали на аппарате высокоэффективной жидкостной хроматографии (ВЭЖХ). Тот же образец использовали для немедленного получения результатов измерений комбинационного рассеяния. С использованием рамановской спектроскопии и алгоритма классических наименьших квадратов на основе модели в супернатантах культуры клеток яичников хомяка, выращенных в колбах в режиме периодической ферментации, с высокой точностью определены концентрации глюкозы и лактата. Библиотека детерминированных спектров комбинационного рассеяния чистых компонентов была создана путем получения спектров комбинационного рассеяния достоверных компонентов питательных сред и метаболитов культур клеток яичников хомяка. В эту библиотеку были включены только анализаторы с концентрациями выше предела обнаружения прибора. Остатки, полученные после анализа классических наименьших квадратов, были использованы для выявления недостающих компонентов и создания исправленной библиотеки. Таким образом, был создан алгоритм для получения подходящей спектральной базы комбинационного рассеяния из сложной химической смеси. Концентрации глюкозы и лактата в супернатантах культуры клеток яичников хомяка определили с помощью рамановской спектроскопии.

Ключевые слова: *Рамановская спектроскопия, биореакторы, классический метод наименьших квадратов, обнаружение глюкозы, обнаружение лактата*